Reactions of Iron Atoms with Nitric Oxide and Carbon Monoxide in Excess Argon: Infrared Spectra and Density Functional Calculations of Iron Carbonyl Nitrosyl Complexes†

Xuefeng Wang,‡ Mingfei Zhou,‡ and Lester Andrews*

University of Virginia, Department of Chemistry, McCormick Road, P.O. Box 400319, Charlottesville, Virginia 22904-4319

Received: February 14, 2000; In Final Form: April 6, 2000

Laser-ablated iron atoms react with CO and NO during condensation in excess argon to produce a series of iron carbonyl nitrosyl complexes. The Fe(CO)(NO), $Fe(CO)_2(NO)$, $Fe(CO)(NO)_2$, and $Fe(CO)_2(NO)_2$ complexes are formed as reaction products during sample deposition and further annealing, which leads to dominance for the saturated $Fe(CO)_2(NO)_2$ complex. The Fe(CO)(NO) complex isomerizes to Fe(CO)(η^2-NO) on visible photolysis and to the isocyanate species OFeNCO on ultraviolet irradiation. The observed absorption bands were identified by isotopic substitution ($^{13}C^{16}O$, $^{15}N^{16}O$, $^{15}N^{18}O$, and mixtures) and reproduced by DFT calculations of vibrational fundamentals. The FeCO subunit observed here in different nitrosyl environments appears to distort and stiffen with an increase in positive charge on iron, which may relate to the deformability of the FeCO subunit in heme proteins. The nature of bonding and reaction mechanism are discussed.

Introduction

The reaction of transition metal atoms with ligands such as CO and NO are of considerable interest in several fields of chemistry such as catalysis, synthesis, and atmospheric chemistry.[1] Recently the interactions between heme iron and NO have been investigated extensively in biochemistry.[2−5] The binding nature of NO and CO with transition metals is very similar; however, NO has an additional antibonding π electron for coordination, which can act as a one or a three-electron ligand, depending on the coordination geometry. Compared to metal carbonyl complexes, which have been widely studied, few works have been done on metal carbonyl nitrosyl complexes. The saturated stable 18-electron iron carbonyl nitrosyl, $Fe(CO)_2(NO)_2$, and its isoelectronic molecule, $Mn(CO)(NO)_3$, have been synthesized, and their structures, spectra, photochemistry, and catalytic properties have been studied.[6−13] The formation and chemistry of unsaturated metal carbonyl nitrosyl complexes remains unclear although evidence has been presented for $Fe(CO)(NO)_2$ from the matrix photochemistry of $Fe(CO)_2(NO)_2$.[10] Such complexes are very important in understanding the bonding in biomolecules and the catalytic process.

Matrix isolation studies of laser-ablated transition-metal atom reactions with CO have been studied intensively in this laboratory, and $M(CO)_x$ complexes, cations, and anions have been observed.[14−19] Recent laser-ablation studies of transition metal reactions with NO have revealed that the NMO insertion product dominates the early metal reactions, but end-bonded nitrosyls M−(η^1-NO)$_x$, and side-bonded M−[η^2-NO] complexes are favored in the later metal reactions.[20−25] The nitrosyls are observed in thermal late metal reactions.[26,27] In this paper we report the reactions of laser-ablated iron atoms with CO and NO mixtures in excess argon during condensation at 10 K. Several iron carbonyl nitrosyls are produced in the low-temperature matrix and identified by isotopic substitution and density functional theory (DFT) calculations.

Experimental Section

The experiment for reactions of laser-ablated metal atoms with small molecules during condensation in excess argon has been described in detail previously.[28,29] The Nd:YAG laser fundamental (1064 nm, 10 Hz repetition rate with 10 ns pulse width) was focused (10 cm fl (fl = focal length)) onto a rotating iron target (Johnson Matthey, 99.98%). The laser energy was varied from 5 to 40 mJ/pulse. Laser-ablated metal atoms were codeposited with nitric oxide and carbon monoxide mixtures (0.2−0.5%) in excess argon onto a 10K CsI cryogenic window at 2−4 mmol/hour for 1 h. Isotopic $^{15}N^{16}O$, $^{13}C^{16}O$, $^{15}N^{18}O$, and selected mixtures, were used in different experiments. Infrared spectra were recorded at 0.5 cm^{-1} resolution on Nicolet 750 with 0.1 cm^{-1} accuracy using an HgCdTe detector. Matrix samples were annealed by warming from 10K to different temperatures as measured by a gold−cobalt vs copper thermocouple, and selected samples were subjected to broadband (λ > 240 nm) photolysis by a medium-pressure mercury arc lamp (Philips, 175W) with globe removed.

Results

Experimental spectra are presented for laser-ablated Fe reactions with NO and CO, and density functional theoretical calculations of metal carbonyl nitrosyl complexes are given for comparison.

Spectra of Fe Reaction Products. Figure 1 shows the spectra of laser ablated iron atom codeposition with 0.2% CO+0.2% NO in argon, and the absorptions are listed in Table 1. After deposition, strong CO (2138.2 cm^{-1}), NO (1871.8 cm^{-1}), and weak $(NO)_2$ (1776.1, 1863.3 cm^{-1}), $(NO)_2^+$ (1589.3 cm^{-1}), NO_2 (1610.8 cm^{-1}), NO_2^- (1243.5 cm^{-1}), and three $(NO)_2^-$ anion isomer absorptions were revealed.[20−25,30] Weak bands at 1922.0, 1748.6, and 1731.5 cm^{-1} have been identified as FeCO, FeNO, and $Fe(NO)_2$, respectively.[14,25,26] New weak absorptions were

† Part of the special issue "C. Bradley Moore Festschrift."

* Author for correspondence. Electronic mail: lsa@virginia.edu.

‡ Permanent address: Laser Chemistry Institute, Fudan University, Shanghai, P. R.China.

10.1021/jp0006025 CCC: $19.00
Published on Web 05/23/2000

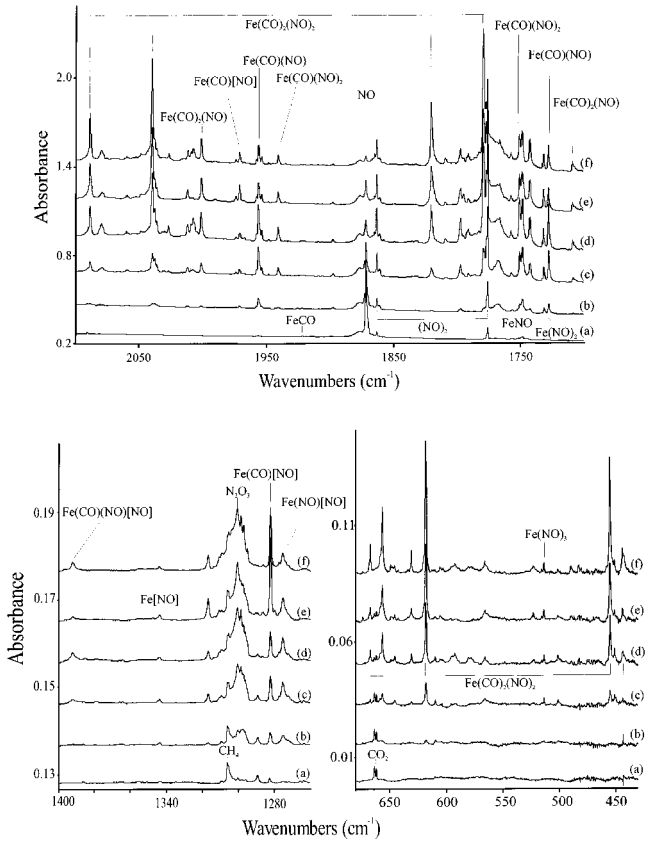

Figure 1. Infrared spectra in the 2100−1700, 1400−1260, and 680−430 cm^{-1} regions for laser-ablated Fe atoms codeposited with 0.2% CO + 0.2% NO in argon at 10 K: (a) after 1 h sample deposit, (b) after annealing to 25 K, (c) after annealing to 30K, (d) after annealing to 35K, (e) after λ > 240 nm photolysis for 10 min, and (f) after annealing to 40K.

observed at 1956.3, 1727.7, and 1282.1 cm^{-1}. Stepwise annealing to 25, 30, and 35 K increased these new absorptions, formed a new group of bands at 2027.0, 2007.8, 1971.2, 1797.6, and 1750.9 cm^{-1}, produced a new set of strong bands at 2089.0, 2039.8, 1820.7, 1779.5, 667.0, 656.6, 630.8, 618.1, and 454.4 cm^{-1}, and decreased the CO and NO absorptions. A 15 min broadband photolysis destroyed the 2027.0, 2007.8, 1956.3, 1797.6, 1750.9, 1748.6, and 1727.7 cm^{-1} absorptions, and increased the new absorptions at 1971.2 and 1282.1 cm^{-1}. A final 40 K annealing slightly decreased 1971.2 and 1282.1 cm^{-1} and further increased other absorptions.

Figure 2 illustrates the carbonyl region and shows the reversible photochemistry of the 1971.2 and 1956.3 cm^{-1} absorptions.

Isotopic $^{13}C^{16}O + {}^{14}N^{16}O$, $^{12}C^{16}O + {}^{15}N^{16}O$, and $^{12}C^{16}O + {}^{15}N^{18}O$ samples and mixtures $^{12}C^{16}O + {}^{13}C^{16}O + {}^{14}N^{16}O$ and $^{12}C^{16}O + {}^{14}N^{16}O + {}^{15}N^{16}O$ were used for molecule identifications through isotopic shifts and splitting of product bands with mixed isotopic samples. The carbonyl and nitrosyl spectral regions are shown in Figures 3 and 4, and the isotopic counterparts are listed in Table 1.

Calculations. The structures and frequencies of expected metal carbonyl nitrosyl products and isomers were calculated with density functional methods using the GAUSSIAN 94 program.[31] The BP86 functional with the 6-311+G(d) basis sets for C, N and O atoms, and the all-electron set of Wachters and Hay as modified for iron in Gaussian were used in the present study.[32−34] The BP86 functional has provided excellent frequency predictions in previous iron carbonyl and nitrosyl

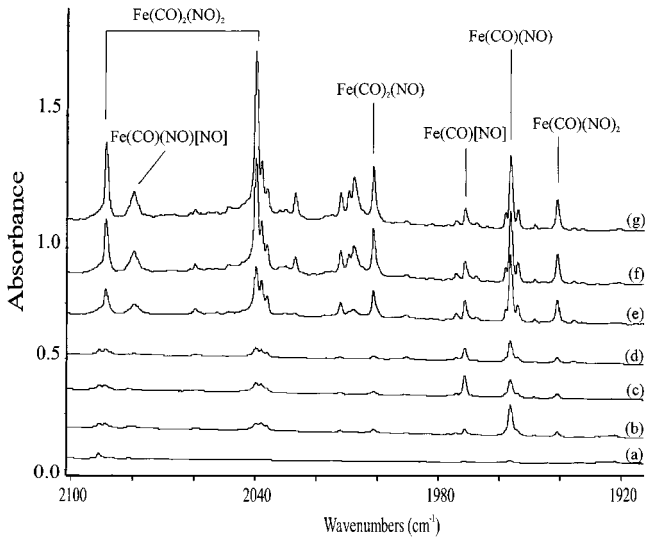

Figure 2. Infrared spectra in the 2100−1920 cm^{-1} carbonyl region for laser-ablated Fe atoms codeposited with 0.2% CO + 0.2% NO in argon at 10 K: (a) after 1 h sample deposit, (b) after annealing to 25 K, (c) after 470−580 nm photolysis for 10 min, (d) after λ > 240 photolysis for 10 min, (e) after annealing to 30 K, (f) after annealing to 35 K, and (g) after annealing to 40 K.

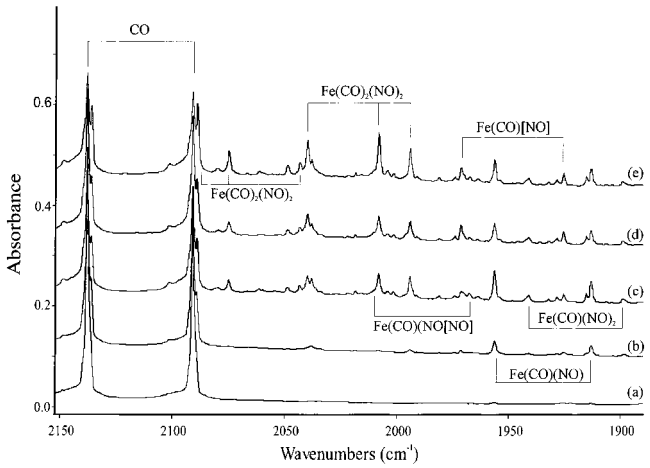

Figure 3. Infrared spectra in the 2150−1900 cm^{-1} carbonyl region for laser-ablated Fe atoms codeposited with 0.1% ^{12}CO + 0.1% ^{13}CO + 0.2% NO in argon at 10 K: (a) after 1 h sample deposit, (b) after annealing to 25 K, (c) after annealing to 35 K, (d) after λ > 240 nm photolysis for 10 min, and (e) after annealing to 40 K.

investigations.[14,25] All geometrical parameters were fully optimized and the harmonic vibrational frequencies were obtained analytically at the optimized structures. The computed structural parameters, relative energies and frequencies, intensities, and isotopic frequency ratios for $Fe(CO)_x(NO)_y$ complexes are summarized in Tables 2 and 3, while Table 4 contains all frequencies calculated for the saturated $Fe(CO)_2(NO)_2$ carbonyl nitrosyl. At optimized BP86/6-311+G(d) geometries, single-point energies were determined at the B3P86 level with the 6-311+G(3df) basis set for comparison.

Four isomers are located on the potential energy hypersurface of the Fe(CO)(NO) molecule. The first one involves end-on bonding of CO and NO ligands. The ground state $^2A'$ is the global minimum at this level of theory, and the $^4A''$ state is 22.8 kcal/mol higher in energy. For the ground state, calculated CO and NO bond lengths are very close to free CO and NO values. The Fe−C and Fe−N distances are 1.778 and 1.653 Å, respectively, and the C−Fe−N angle is 121.5°. The second isomer, Fe(CO)[NO], is also known as Fe(CO)(η^2-NO), and

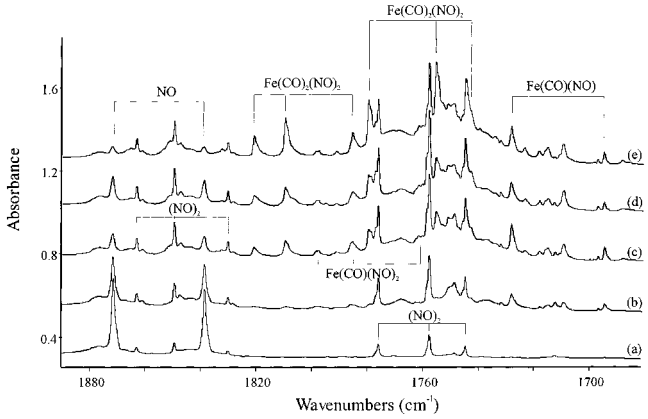

Figure 4. Infrared spectra in the 1890−1680 cm^{-1} nitrosyl region for laser-ablated Fe atoms codeposited with 0.2% CO + 0.1% ^{14}NO + 0.1% ^{15}NO in argon at 10 K: (a) after 1 h sample deposit, (b) after annealing to 25 K, (c) after annealing to 35K, (d) after $\lambda > 240$ nm photolysis for 10 min, and (e) after annealing to 40 K.

three states are located. The $^2A'$ configuration is the ground state, which is 10.1 kcal/mol higher in energy than the ground state of Fe(CO)(NO). The bond length of NO, 1.256 Å, is longer than that of free NO due to side-on interaction with the Fe atom. For the third isomer OFeNCO, the almost linear $^2A'$ ground state is only 1.1 kcal/mol above Fe(CO)(NO). The fourth isomer NFeO(CO), also described as CO bonded to Fe in NFeO, the $^2A'$ ground state is 15.2 kcal/mol higher in energy than the ground state of Fe(CO)(NO).

Calculations were performed for $Fe(CO)_2(NO)_2$, $Fe(CO)_2$-(NO), and $Fe(CO)(NO)_2$, and the results are also listed in Table 2. Saturated $Fe(CO)_2(NO)_2$ was predicted to have a $^1A_1$ ground state with C_{2v} symmetry, and the calculated parameters are in excellent agreement with the microwave structure determination.[9] The bond lengths are overestimated by 0.01−0.02 Å, and the discrepancy in bond angles ranges from 0.7 to 2.5°. Both $Fe(CO)(NO)_2$ and $Fe(CO)_2(NO)$ are calculated to have C_s symmetry and the ground states $^1A'$ and $^2A''$, respectively.

Discussion

The new reaction product absorptions will be identified and assigned on the basis of annealing and photolysis behavior, isotopic substitution, and DFT isotopic frequency calculations. Several known $Fe(CO)_x$ and $Fe(NO)_y$ species prepared in earlier experiments[14,25,26] are listed in Table 1.

Fe(CO)(NO). The new carbonyl and nitrosyl absorptions at 1956.3 and 1727.7 cm^{-1} can be assigned to the new Fe(CO)-(NO) complex. The two bands increased together on annealing to 25, 30, and 35K, but decreased on broadband photolysis. The 1956.3 cm^{-1} band shows a 43.4 cm^{-1} ^{13}CO isotopic shift, but only a 1.3 cm^{-1} ^{15}NO isotopic shift. The $^{12}CO/^{13}CO$ isotopic ratio 1.02269 and $^{14}NO/^{15}NO$ ratio 1.00066 suggest that this band is due to a terminal C−O stretching vibration with very small coupling to nitrogen. The 1727.7 cm^{-1} band exhibits a small 1.7 cm^{-1} ^{13}CO isotopic shift but large 33.8 cm^{-1} ^{15}NO and 70.2 cm^{-1} $^{15}N^{18}O$ isotopic shifts. The $^{14}NO/^{15}NO$ isotopic ratio 1.01995 and $^{15}N^{16}O/^{15}N^{18}O$ isotopic ratio 1.02196 indicate that this band is due to a terminal N−O stretching vibration with little involvement of carbon. Only one CO as well as one NO subunit participate in these modes according to the doublet isotopic structures observed in mixed $^{12,13}CO$ + NO and CO + $^{14,15}NO$ experiments (Figures 3 and 4).

The assignment is further confirmed by DFT calculations summarized in Table 3 for the $^2A'$ ground state. The C−O stretching frequency is calculated at 1957.9 cm^{-1}, only 1.6 cm^{-1} higher than the observed value. The calculated N−O stretching frequency, 1753.7 cm^{-1}, is 26 cm^{-1} higher than the observed value. This agreement is expected for the pure density functional.[14,25] The predicted relative intensities (750/989 = 0.76) and isotopic frequency ratios agree very well with experimental observations; the observed intensity ratio is 0.83 and deviations of 0.05% ($^{13}CO/^{12}CO$) and 0.02% ($^{15}NO/^{14}NO$), respectively (Tables 1 and 3), are found in the isotopic frequency ratios.

Fe(CO)[NO] or Fe(CO)(η^2- NO). The sharp bands at 1971.2 and 1282.1 cm^{-1} exhibit the same profile, slightly increase together on annealing to 25, 30, and 35 K, greatly increase on visible or broadband photolysis at the expense of Fe(CO)(NO), and decrease on further annealing to 40 K, suggesting that they are due to different modes of the same molecule. Figure 2 shows that $\lambda > 470$ nm visible photolysis *reduces* Fe(NO)(CO) by half and *increases* the 1971.2 cm^{-1} band 3-fold, then $\lambda > 240$ nm photolysis reduces the 1971.2 cm^{-1} band by half and increases Fe(CO)(NO) by 20%. Further annealing to 30K increases Fe(CO)(NO) in greater proportion than the 1971.2 cm^{-1} absorption. The ^{13}CO counterpart for the 1971.2 cm^{-1} band appears at 1925.1 cm^{-1}, gives the $^{12}CO/^{13}CO$ isotopic ratio 1.02349, which is slightly higher than the value 1.02274 for Fe(CO)(NO). The 1282.1 cm^{-1} band in the η^2-NO complex region[25,27] shifted to 1260.5 cm^{-1} in ^{15}NO experiments, which gives the 1.01714 isotopic $^{14}NO/^{15}NO$ ratio, and 1226.4 cm^{-1} with $^{15}N^{18}O$ and the 1.02780 $^{15}N^{16}O/^{15}N^{18}O$ ratio. In mixed $^{12,13}CO$ + NO and CO + $^{14,15}NO$ isotopic spectra, doublets with 1:1 distribution were observed for both bands. These two bands are assigned to the Fe(CO)(η^2-NO)complex.

This identification is strongly supported by the DFT calculated frequencies presented in Table 3. For the $^2A'$ ground state, the stretching modes of C−O and N−O are calculated to be 1969.4 cm^{-1} with the 1.02445 $^{12}CO/^{13}CO$ isotopic ratio and 1332.5 cm^{-1} with the 1.01780 $^{14}NO/^{15}NO$ isotopic ratio, respectively, which are in excellent agreement with observed frequencies and isotopic ratios. The η^2-NO subunit is clearly more difficult to model by theory.

$Fe(CO)(NO)_2$ and Fe(CO)(NO)[NO]. The band at 1940.9 cm^{-1} tracks with the 1797.6 and 1750.9 cm^{-1} absorptions, and all three are assigned to $Fe(CO)(NO)_2$. These three bands appear on annealing to 25K after Fe(CO)(NO) absorptions, increase on further annealing to 30 and 35K, and slightly decrease on photolysis. The 1940.9 cm^{-1} band exhibits the carbonyl stretching isotopic ratio ($^{12}CO/^{13}CO$, 1.02223) and a 1:1 doublet at 1940.9 and 1898.6 cm^{-1} in the mixed $^{12,13}CO$ + NO experiment, indicating that only one carbonyl is involved. The 1797.6 and 1750.9 cm^{-1} bands shifted to 1762.5 and 1715.5 cm^{-1}, respectively, with ^{15}NO + CO sample. The 1797.6 cm^{-1} band shows a 1:2:1 triplet in the $^{14,15}NO$ + CO experiment, but the mixed isotopic multiplet for the 1750.9 cm^{-1} band is overlapped by absorption bands due to $Fe(NO)_x$ species.[25]

Three bands at 2079.8, 1791.2, and 1392.3 cm^{-1} increased on annealing but decreased on photolysis. The 2079.8 cm^{-1} band shifted to 2034.0 cm^{-1} in the ^{13}CO + NO experiments, and a doublet with 1:1 relative intensities was observed in mixed $^{12,13}CO$ + NO spectra for this band. The 1791.2 and 1368.5 cm^{-1} bands showed 1:1 doublet shape in the CO+$^{14,15}NO$ spectra, but their 14/15 isotopic ratios were 1.02005 and 1.01739, respectively, indicating two different NO subunits are invoved in this molecule. The 1791.2 cm^{-1} band has the behavior of NO end-on coordinated to the metal, while the 1392.3 cm^{-1} band showed the character of side-on NO bonded

TABLE 1: Absorptions (cm^{-1}) from Codeposition of Laser-Ablated Fe Atoms with NO and CO in Argon at 10 K

CO + NO	^{13}CO + NO	CO+^{15}NO	CO+^{15}N^{18}O	^{12,13}CO + NO	CO+^{14,15}NO	^{12}CO/^{13}CO	^{14}NO/^{15}NO	assignment
2254.5	2193.6	2240.6	2240.0	2254.4, 2183.6	2254.5, 2240.6	1.02776	1.00620	OFeNCO site
2248.2	2187.9	2234.1	2233.8	2248.2, 2187.9	2248.2, 2234.1	1.02756	1.00631	OFeNCO
2244.4	2184.0	2229.0	2229.0	2244.4, 2184.0	2244.4, 2228.9	1.02766	1.00691	OFeNCO site
2138.2	2091.1	2138.2	2138.2	2138.2, 2091.1	2138.2	1.02252		CO
2089.0	2043.3	2087.7	2086.6	2089.0, 2075.1, 2043.3		1.02237	1.00062	$Fe(CO)_2(NO)_2$
2079.8	2034.0	2079.1				1.02252	1.00034	Fe(CO)(NO)[NO]
2050.0	2004.1			2048.8		1.02290		$(Fe(CO)_2(NO))$?
2039.8	1994.1	2039.8	2040.0	2039.8, 2008.0, 1994.0		1.02292		$Fe(CO)_2(NO)_2$
2036.2	1991.2	2036.2		2036.2, 1991.2	2036.2	1.02260		OFeCO
2027.0	1981.2	2027.0				1.02312		?
2012.0	1967.0	2012.0				1.02288		?
2007.8	1963.3	2007.8				1.02267		$Fe_x(CO)_y$
2001.5	1957.0	2001.4	2001.4	1981.1		1.02274		$Fe(CO)_2(NO)$
1971.2	1925.2	1971.1	1970.9	1971.2, 1925.1		1.02389		Fe(CO)[NO]
1956.3	1912.9	1955.0	1954.0	1956.3, 1912.9	1956.3, 1955.0	1.02269	1.00066	Fe(CO)(NO)
1940.9	1898.7	1940.8	1940.8	1941.0, 1898.6		1.02223		$Fe(CO)(NO)_2$
1922.0	1876.2	1922.0	1921.9	1922.0, 1876.2	1922.0	1.0244		FeCO
1871.8	1871.8	1839.0	1789.3	1871.8	1871.8, 1839.0		1.01784	NO
1863.3	1863.3	1830.4	1781.2					$(NO)_2$
1820.7	1819.2	1785.1	1746.0		1820.7, 1809.6, 1785.2	1.00082	1.01994	$Fe(CO)_2(NO)_2$
1809.5	1808.7	1773.5				1.00044	1.02030	?
1797.6	1795.7	1762.5	1724.2	1797.6	1797.6, 1795.7, 1759.0	1.00106	1.01991	$Fe(CO)(NO)_2$
1791.2	1791.2	1756.0	1716.7				1.02005	Fe(CO)(NO)[NO]
1779.5	1779.5	1744.0	1704.9		1779.5, 1775.1, 1744.1		1.02036	$Fe(CO)_2(NO)_2$
1776.1	1776.1	1744.2	1697.4		1776.1, 1757.5, 1744.2	1.01829		$(NO)_2$
1750.9	1750.8	1715.5	1676.6		1750.8, 1730.6, 1715.8		1.02064	$Fe(CO)(NO)_2$
1748.6	1748.5	1714.5			1748.6, 1714.5		1.01989	Fe(NO)
1742.4	1742.4	1708.7	1668.6				1.01972	$Fe(NO)_3$
1731.5	1731.5	1696.2	1659.7		1731.5, 1709.0, 1696.2		1.01081	$Fe(NO)_2$
1727.7	1726.0	1693.9	1657.5	1727.7, 1726.1	1727.7, 1693.9	1.00098	1.01995	Fe(CO)(NO)
1708.7	1708.4	1677.0	1634.8			1.00018	1.01890	$Fe(CO)_2(NO)$
1392.3	1392.2	1368.5	1332.9		1392.1, 1368.7		1.01739	Fe(CO)(NO)[NO]
1343.8	1343.7	1321.4	1284.8				1.01695	Fe[NO]
1316.7	1316.6	1293.9			1316.7, 1293.9		1.01762	$Fe(CO)_x$[NO]
1282.1	1281.9	1260.5	1226.4	1282.1	1282.1, 1260.5		1.01714	Fe(CO)[NO]
1275.3	1275.4	1252.6	1219.1		1274.7, 1253.5		1.01812	Fe(NO)[NO]
966.7	966.7	949.7	940.9		966.7, 949.7		1.01790	$NFeO(CO)_x$?
949.9	949.8	933.6	923.8		949.9, 933.6		1.01746	NFeO(CO)?
942.7	942.7	926.8	916.9		942.6, 926.8		1.01716	NFeO?
941.3	941.3	925.7	915.5		941.3, 925.7		1.01685	site
925.9	925.9	925.7						anneal pdt
915.5	915.3	915.4	876.5					OFeNCO
894.9	894.9	894.9						phot pdt
872.8	872.8	872.8	834.5					FeO, OFeCO
673.7	673.7	671.3					1.00358	Fe_xNO
667.0	661.3	661.9		667.0, 662.6, 661.3		1.00862	1.00771	$Fe(CO)_2(NO)_2$
656.6	652.8	644.9	641.1	656.6, 652.6	656.6, 651.0, 644.9	1.00582	1.01814	$Fe(CO)_2(NO)_2$
630.8	623.7	621.0	616.6	630.8, 627.0, 623.6	630.9, 626.8, 624.7	1.01138	1.01578	$Fe(CO)_2(NO)_2$
618.1	613.8	607.1	604.5	618.1, 616.1, 613.8	618.1, 612.7, 607.0	1.00701	1.01812	$Fe(CO)_2(NO)_2$
513.3	513.3	499.8			512.9, 508.1, 505.0, 500.2		1.02641	$Fe(NO)_3$
454.4	443.5	451.8	450.0	454.4, 448.2, 443.5	454.4, 453.0, 452.0	1.02458	1.00575	$Fe(CO)_2(NO)_2$
443.5	438.3	442.9	441.9			1.01186	1.00135	$Fe(CO)_2(NO)_2$

to a metal atom.[25,27] These three bands are appropriate for the Fe(CO)(NO)[NO] molecule.

Similar DFT calculations were done for these two isomers, and the results are listed in Tables 2 and 3. The assignment is supported by calculations, which reproduce very well the observed isotopic ratios but the predicted frequencies have 20−60 cm^{-1} deviations from the experimental observations, slightly more than Fe(CO)(NO). The calculations predicted $Fe(CO)(NO)_2$ with C_s symmetry slightly lower in energy than Fe(CO)(NO)[NO]. Note that the calculated FeCO angles in the two molecules are close to 180°, but the CO stretching mode for $Fe(CO)(NO)_2$ is slightly lower than that for Fe(CO)(NO)[NO], which indicates that the bonding of CO coordinated to Fe is stronger in $Fe(CO)(NO)_2$ than in Fe(CO)(NO)[NO].

It is interesting to compare the electronic configurations, Mulliken charge distributions and frequencies of FeCO subunits in the series of complexes in Table 5. The FeCO molecule is calculated to be linear with a $^3\Sigma^-$ ground state, which is consistent with the results predicted at several levels of theory[35−41] and experiments.[42,43] However, the Fe−CO bond is weakened upon coordination of NO ligands. As a result the νFe−C stretching mode is redshifted while the νC−O stretching and δFeCO bending modes are blue shifted. In FeCO, σ donation from the 5σ molecular orbital of CO contributes to the unoccupied Fe orbital of σ symmetry(dσ), while the π back-donation is from the 3dπ(Fe) orbital to the empty antibonding orbital (2π*) of CO. The 3dπ(Fe) orbital is oriented to Fe−C bond with optimized π-overlap. However, the 3dπ(Fe)-2π*-(CO) interaction is reduced since both of the charge distribution of Fe atom and orientation of the 3dπ(Fe) orbital are strongly perturbed by Fe−N bonding. Therefore, the bent ∠FeCO structures are obtained due to different NO number and bonding style. As seen in Table 5, as the positive charge on Fe increases, FeCO angles decrease, and the δFeCO bending modes blueshift.

This trend can be used to understand the distorted FeCO unit in heme-Fe−CO structures. The crystal structures of the

TABLE 2: Iron Carbonyl Nitrosyl States, Relative Energies (kcal/mol), and Geometries Calculated at the BP86/6-311+G(d) Level

molecule	state	relative energy	geometry (*D*, deg)
Fe(CO)(NO) (C_s)	$^2A'$	0.0 (0.0)[a,b]	CO,1.168; FeC,1.778; NO,1.185 FeN,1.653; FeCO,172.0; FeNO,159.2; CFeN,121.5
	$^4A''$	22.8 (27.2)[a]	CO,1.165; FeC,1.806; NO,1.192; FeN,1.702; FeCO,176.3; FeNO,173.0; CFeN,110.1
Fe(CO)[NO]	$^2A'$	10.1 (7.1)[a]	CO,1.168; FeC,1.765; NO,1.256; FeN,1.732; FeO,1.986; FeCO,177.1; FeNO,81.7; OFeN,38.7
	$^4A'$	27.4 (19.2)[a]	CO,1.166; FeC,1.816; NO,1.259; FeN,1.829; FeO,1.981; FeCO,180.0; FeNO,77.4; OFeN,38.3
	$^6A'$	45.2 (22.6)[a]	CO,1.162; FeC,1.823; NO,1.292; FeN,1.955; FeO,2.008; FeCO,180.0; FeNO,73.2; OFeN,38.0
OFeNCO	$^2A'$	1.1	OFe, 1.593; FeN, 1.817; NC, 1.220; CO, 1.180; OFeN, 179.3; FeNC, 180.0; NCO, 180.0
NFeO(CO)	$^2A'$	15.2 (31.6)[a]	CO,1.148; FeC,1.846; NO,2.874; FeN,1.548; FeO,1.605; FeCO,179.2; OFeN,130.6
	$^4A'$	44.1 (53.8)[a]	CO,1.144; FeC,1.932; NO,2.681; FeN,1.593; FeO,1.640; FeCO,180.0; OFeN,115.9
$Fe(CO)(NO)_2$ (C_{2v})	$^1A_1$	0.0 (0.0)[a,c]	CO,1.152; NO,1.175; FeN,1.652; FeC,1.891; FeCO,180.0; NFeN,115.5
Fe(CO)(NO)[NO]	^1A	18.6 (14.7)[a]	CO,1.158; NO,1.176; NO′,1.246; FeC,1.801; FeN,1.676; FeN′,1.768
$Fe(CO)_2(NO)$[d] (C_s)	$^2A''$		CO,1.161; FeC,1.803; NO,1.179; FeN,1.664; FeNO,158.1; FeCO,179.9; CFeC,92.8; CFeN,112.7

[a] Single-point energies at B3P86/6-311+G(3df) level for BP86 optimized geometries in parentheses. [b] Dissociation energy of complex is 81.3 kcal/mol from eq 1+3 or 2+4. [c] Dissociation energy of complex is 122.5 kcal/mol from eq 1+3+8. [d] Dissociation energy of $Fe(CO)_2(NO)$ is 109.5 kcal/mol from eq 1+3+7; dissociation energy of $Fe(CO)_2(NO)_2$ is 165.3 kcal/mol from eq 1+3+7+10.

TABLE 3: Stretching Frequencies (cm^{-1}) and Intensities (km/mol) for Isotopic C−O and N−O Vibrations Calculated at the BP86/6-311+G(d) Level for Ground State Iron Carbonyl Nitrosyls

molecule	mode	^{12}CO, ^{14}NO	^{13}CO, ^{14}NO	^{12}CO, ^{15}NO	($^{12}CO/^{13}CO$)	($^{14}NO/^{15}NO$)
Fe(CO)(NO)	C−O	1957.9(750)	1913.6(643)	1956.7(794)	1.02315	1.00010
	N−O	1753.7(989)	1752.0(1040)	1719.1(914)	1.00097	1.02013
Fe(CO)[NO]	C−O	1969.4(775)	1922.4(730)	1969.3(776)	1.02445	1.00005
	N−O	1332.5(322)	1332.5(323)	1309.2(314)	1.00000	1.01780
OFeNCO	N−C−O, a	2236.3(1469)	2174.2(1407)	2225.4(1435)	1.02856	1.00490
	N−C−O, s	1388.4(39)	1388.0(37)	1360.4(42)	1.00029	1.02058
	Fe−O	931.8(136)	931.8(135)	931.8(36)	1.00000	1.00000
NFeO(CO)	C−O	2077.8(576)	2029.3(544)	2077.7(576)	1.02390	1.00000
	Fe−N	1060.2(99)	1060.2(97)	1034.4(109)	1.00000	1.02494
	Fe−O	949.1(75)	949.1(75)	946.4(62.3)	1.00000	1.00285
$Fe(CO)(NO)_2$ (C_{2v})	C−O	2002.7(635)	1958.9(518)	2000.8(688)	1.02236	1.00095
	N−O, s	1818.9(757)	1816.2(824)	1783.2(683)	1.00149	1.02002
	N−O, as	1771.3(1300)	1771.3(1300)	1735.4(1246)	1.00000	1.02069
Fe(CO)(NO)	C−O	2033.0(661)	1987.9(605)	2032.3(675)	1.02269	1.00034
[NO]	N−O	1778.1(856)	1777.2(870)	1743.5(810)	1.00051	1.01985
	[N−O]	1369.2(350)	1369.1(351)	1344.6(341)	1.00001	1.01845
$Fe(CO)_2(NO)$	C−O, s	2009.5(327)	1964.1(267)	2008.1(359)	1.02311	1.00070
	C−O, as	1947.5(1099)	1902.2(1035)	1947.4(1099)	1.02381	1.00005
	N−O	1772.5(995)	1770.9(1026)	1737.3(930)	1.00090	1.02026

myoglobin CO adduct reveal a large off-axis distortion,[44,45] which is believed to be due to interaction between Fe and the imidazole ring. Further experimental and theoretical studies also support this result.[46−49] However, distorted FeCO is not supported by infrared polarization measurement.[50,51] From this study it appears that the positive charge distribution on Fe atom and N-containing ligands may directly affect the Fe−CO unit bonding in heme-CO adducts.

$Fe(CO)_2(NO)_2$. The dominant bands after annealing and photolysis appear at 2089.0, 2039.8, 1820.7, and 1779.5 cm^{-1} in the carbonyl and nitrosyl regions and at 667.0, 656.6, 630.8, 618.1, 454.4, and 443.5 cm^{-1} in the lower region. The upper 2089.0 and 2039.8 cm^{-1} pair shows carbonyl stretching frequency ratios and triplets with 1:2:1 intensity distribution for both bands in the $^{12,13}CO + NO$ experiment, which are appropriate for symmetric and antisymmetric modes of two carbonyl subunits. These bands are 104.2 and 160.6 cm^{-1}, respectively, higher than the two C−O vibrational frequencies of bent $Fe(CO)_2$ in an argon matrix.[14] The two lower bands at 1820.7 and 1779.5 cm^{-1} exhibit the same profile and increase together with the upper pair. The lower bands shift to 1785.1 and 1744.0 cm^{-1} with ^{15}NO and to 1746.0 and 1704.9 cm^{-1} with $^{15}N^{18}O$, and show triplets with 1:2:1 intensity using $^{14,15}NO + CO$ sample, indicating that two nitrosyl subunits participate. These bands are 22.6 and 47.9 cm^{-1} higher, respectively, than the two bands for bent $Fe(NO)_2$ in solid argon.[25] In addition these four strong bands are within 1 cm^{-1} of the spectrum measured for an authentic sample of $Fe(CO)_2(NO)_2$ in solid argon, but there is no report of lower frequency modes.[10]

In addition, three strong lower frequency bands observed here at 656.6, 618.1, and 454.4 cm^{-1} track very well with the four upper bands. The 656.6 and 618.1 cm^{-1} bands show very small carbon isotopic shifts but large nitrogen isotopic shifts, with triplets in both $^{12,13}CO + NO$ and $^{14,15}NO + CO$ experiments, and are due to FeNO bending/Fe−N stretching modes. On the other hand, the 454.4 cm^{-1} band shifts a large amount to 443.5 cm^{-1} in ^{13}CO experiments (1.02458 $^{12}CO/^{13}CO$ isotopic ratio), which is due to an FeCO bending/Fe−C stretching vibration. The weaker 667.0 cm^{-1} band has similar small isotopic ratios for $^{12}CO/^{13}CO$ and $^{14}NO/^{15}NO$, indicating that bending of both FeCO and FeNO subunits is involved with considerable oxygen motion. The weaker 443.5 cm^{-1} band appears to be more FeCO bending in character. The remaining weak 630.8 cm^{-1} absorption is probably due to a combination band.

The experimental results for $Fe(CO)_2(NO)_2$ are modeled well by DFT calculations of frequencies and vibrational mode assignments. The calculated and observed frequencies and isotopic ratios are summarized in Table 4. The calculation predicts very strong symmetric and antisymmetric stretching C−O and N−O vibrations, as well as medium intensity FeNO bending and weak FeCO bending modes. Note that the

TABLE 4: Calculated and Experimental Frequencies, Intensities, and Isotopic Frequency Ratios at the BP86/6-311+G(d) Level for $Fe(CO)_2(NO)_2$ ($^1A_1$) in C_{2v} Symmetry

	calculated			experimental			
symmetry	frequencies (cm^{-1}) (km/mol)	($^{12}C/^{13}C$)	($^{14}N/^{15}N$)	frequencies (cm^{-1}) (au)	($^{12}C/^{13}C$)	($^{14}N/^{15}N$)	assignments
a_1	2047.2(345)	1.02263	1.00083	2089.0(0.151)	1.02237	1.00062	CO sym str
	1840.8(801)	1.00131	1.02012	1820.7(0.206)	1.00082	1.01994	NO sym str
	684.5(82)	1.00117	1.01906	656.6(0.014)	1.00582	1.01814	FeNO bend(out)
	583.7(1)	1.00154	1.01566				NFeN str
	510.5(14)	1.02903	1.00275				FeCO bend(in)
	438.0(2)	1.01459	1.00206				(CO)Fe(CO) bend
	82.7(0)	1.00242	1.00121				OCFeCO bend
	65.2(0)	1.00308	1.00806				CFeC bend
a_2	498.3(0)	1.01363	1.01735				torsion
	328.2(0)	1.01989	1.01078				FeNO(out)FeCO(in)
	68.5(0)	1.00293	1.00146				OCFeCO bend(out)
b_1	1999.0(976)	1.02376	1.00000	2039.8(0.322)	1.02292	1.00000	CO antisym str
	663.5(100)	1.00515	1.01717	618.1(0.020)	1.00701	1.01812	FeNO bend
	482.0(10)	1.01175	1.00396	443.5(0.005)	1.01186	1.00135	FeCO bend(out)
	333.1(1)	1.02492	1.00000				CFeC str
	74.0(0)	1.00407	1.00135				ONFeNO bend(out)
b_2	1806.0(1377)	1.0000	1.02068	1779.5(0.442)	1.00000	1.02036	NO antisym str
	664.3(14)	1.00045	1.00621	667.0(0.007)	1.00862	1.00771	FeNO/FeCO bending
	501.5(14)	1.02431	1.00723	454.4(0.017)	1.02458	1.00575	FeCO bend(out)
	291.0(0)	1.00727	1.02069				FeNO(in)FeCO(out)
	85.3(0)	1.00000	1.00235				torsion

TABLE 5: Summary of Frequencies (cm^{-1}) of the NBO Analysis and Calculated C−O Stretching, Fe−C Stretching, and FeCO Bending Frequencies in the $(NO)_xFeCO$ Complexes

molecule	Fe electronic configuration	C electronic configuration	q_{Fe}	q_C	∠FeCO	$\nu_{C-O}(\sigma)$	$\nu_{Fe-CO}(\sigma)$	$\delta_{Fe-C-O}(\pi)$
Fe(CO)	$4s^{0.83}3d^{7.01}$	$2s^{1.27}2p^{2.37}$	−0.0936	0.3147	180.0	1921.4	569.7	356.8
Fe(CO)[NO]	$4s^{0.35}3d^{7.12}$	$2s^{1.33}2p^{2.30}$	0.0949	0.2239	177.1	1969.4	473.9	571.4
Fe(CO)(NO)	$4s^{0.40}3d^{7.17}$	$2s^{1.35}2p^{2.32}$	0.0997	0.2041	172.0	1957.9	513.4	582.9[a]
$Fe(CO)(NO)_2$	$4s^{0.37}3s^{7.20}$	$2s^{1.36}2p^{2.33}$	0.4364	0.1906	170.1	2002.7	321.4	600.3[a]

[a] Weakly coupled with FeNO bending mode.

calculated C−O stretching modes are 41.8 and 40.8 cm^{-1} lower (2.0%) than observed while the calculated N−O stretching modes are 20.1 and 26.5 cm^{-1} higher (1.1 and 1.5%) than the observed values. The calculated 684.5 and 663.5 cm^{-1} bands as well as their isotopic ratios are very close to the experimental absorptions at 656.6 and 618.1 cm^{-1} and the observed isotopic ratios, respectively. These two bands are due to FeNO bending modes with in-plane and out-of-plane character, respectively. The calculated out-of-plane FeCO bending mode at 501.5 cm^{-1} is slightly higher than the experimental absorption at 454.4 cm^{-1}. The predicted out-of-plane bending mode of FeCO at 482.0 cm^{-1} matches the very weak absorption at 443.5 cm^{-1}. The calculated Fe−N and Fe−C stretching modes are mixed and their infrared intensities are very small.

$Fe(CO)_2(NO)$. The 2001.5 and 1708.7 cm^{-1} bands increased markedly on annealing and shifted to 1957.0 and 1708.4 cm^{-1}, respectively, in the ^{13}CO + NO sample. But in the mixed $^{12,13}CO$ + NO experiment no isotopic multiplet could be identified due to overlap by bands of other carbonyls. The 1708.7 cm^{-1} band shifted to 1677.0 cm^{-1} and showed a 1:1 doublet pattern in CO+$^{14,15}NO$ spectra, indicating one NO subunit. The 2001.5 cm^{-1} band is red shifted from C−O vibrations of $Fe(CO)_2(NO)_2$ and blue-shifted from $Fe(CO)_2$ in an argon matrix.[14] So $Fe(CO)_2(NO)$ is an appropriate candidate; a weaker 2050.0 cm^{-1} band may be associated but we cannot be certain. However, from DFT calculation the predicted NO stretching mode of $Fe(CO)_2(NO)$ molecule at 1772.5 cm^{-1} is higher than the 1708.7 cm^{-1} experimental value, which is not as good agreement as the other nitrosyl modes assigned here. Clearly, evidence for the identification of $Fe(CO)_2(NO)$ is not as strong as for the other five iron carbonyl nitrosyls reported here.

Other Absorptions. Several absorptions remain to be discussed. The 2007.8 cm^{-1} band is observed with Fe and CO and is there identified as $Fe_x(CO)_y$.[14] Two weak new carbonyl bands at 2027.0 and 2012.0 cm^{-1} are unidentified; the latter appears on earlier annealing and the former is photosensitive. Either of these bands could be due to the unsaturated $Fe(CO)_3(NO)$ species, but this is only one possibility. The OFeCO species made in the Fe/CO_2 reaction[52] appears here at 2036.2 and 872.8 cm^{-1} on annealing from the union of FeO and CO.

Finally, new weak bands observed at 2254.5, 2248.2, and 2244.4 cm^{-1} on photolysis and annealing are analogous to bands in this region from the Mn/CO/NO reaction,[53] and to isocyanate absorptions on supported metal systems.[54−57] These bands have a unique high $^{12}CO/^{13}CO$ ratio (1.027) and low $^{14}NO/^{15}NO$ ratio (1.006) which shows more carbon motion than a normal carbonyl mode plus some nitrogen motion. Our DFT calculations predicted a stable OFeNCO isomer, only 1.1 kcal/mol higher than Fe(CO)(NO), with very strong antisymmetric N−C−O stretching mode at 2236.3 cm^{-1} and weak Fe−O mode at 931.8 cm^{-1}. An experiment with $^{12}C^{16}O$ and $^{15}N^{18}O$ was performed just to show that oxygen in the FeO subunit arises from NO and the $^{18}OFe^{15}N^{12}C^{16}O$ isotopic molecule was formed exclusively. The 2254.5, 2234.1, and 2228.9 cm^{-1} bands with $^{15}N^{16}O$ redshifted 0.0−0.6 cm^{-1} with $^{15}N^{18}O$ substitution, but the band at 915.5 cm^{-1} shifted to 876.5 cm^{-1} (ratio 1.04495) as is appropriate for an Fe−O stretching mode. This observation of an iron isocyanate species from one Fe, one CO, and one NO is relevant to reactions of CO and NO on supported metal catalyst systems for pollution control.[54−57]

Reaction Mechanisms. Both FeNO and FeCO can be formed by direct reaction during matrix deposition, but NO, with one unpaired electron in a π^* orbital, is more reactive than CO.

Reactions 1 and 2 are exothermic by 39.1 and 21.0 kcal/mol, respectively, based on B3P86/6-311+G(3df) calculated energies. On annealing the FeNO absorption increased while

$$Fe(^5D) + NO(^2\Pi) \rightarrow Fe(NO)\ (^2A') \qquad \Delta E = -39.1 \text{kcal/mol} \quad (1)$$

$$Fe(^5D) + CO(^1\Sigma^+) \rightarrow Fe(CO)\ (^3\Sigma^-) \qquad \Delta E = -21.0 \text{kcal/mol} \quad (2)$$

the FeCO absorption disappeared. This means that the ground-state Fe(^{5}D) atom can react with NO to form FeNO without energy barrier but not with CO to form FeCO in solid argon. This result agrees with our previous studies of reactions of iron atoms with CO in solid argon and neon.[14,17]

The Fe(CO)(NO) molecule is mainly produced from reaction 3 during annealing. Although reaction 4 is more exothermic, the yield of FeCO is limited in the argon matrix. It is interesting

$$Fe(NO)(^2A') + CO\ (^1\Sigma^+) \rightarrow Fe(CO)(NO)(^2A') \qquad \Delta E = -42.2 \text{kcal/mol} \quad (3)$$

$$Fe(CO)(^3\Sigma^-) + NO(^2\Pi) \rightarrow Fe(CO)(NO)(^2A') \qquad \Delta E = -60.3 \text{kcal/mol} \quad (4)$$

$$Fe(NO)(^2A') + NO(^2\Pi) \rightarrow Fe(NO)_2\ (^1A_1) \qquad \Delta E = -44.2 \text{kcal/mol} \quad (5)$$

to note that reactions 3 and 5 are exothermic by almost the same amount despite very different ligands, CO and NO, coordinating to FeNO. From the theoretical structure (BP86/6-311+G* level) the FeNO angle in Fe(NO)$_2$ (^{1}A$_1$) is 160.6°, while this angle is close to 180° in iron mononitrosyl (178.7°). This means that σ antibonding repulsion in Fe(NO)$_2$ (^{1}A$_1$) molecule from the interaction of 5σ MO of NO and the d$_\sigma$ orbital of the metal center is very strong, which partly eliminates the electron pairing energy from NO π* and Fe 3d$_\pi$. However, this repulsion is small due to no σ antibonding interaction in the Fe(CO)(NO) (^{2}A′) molecule.

The Fe(CO)[NO] absorption bands increased markedly on visible ($\lambda >$ 470 nm) photolysis at the expense of Fe(CO)(NO), suggesting photochemical isomerization of Fe(CO)(NO) to form Fe(CO)[NO]. A following full arc ($\lambda >$ 240 nm) photolysis restored some of the original Fe(CO)(NO) at the expense of Fe(CO)[NO] (Figure 2).

$$\underset{E = 0.0}{Fe(CO)(NO)(^2A')} \underset{\lambda > 240\ nm}{\overset{\lambda > 470\ nm}{\rightleftharpoons}} \underset{E = 10.1}{Fe(CO)[NO](^2A')} \xrightarrow{\lambda > 240\ nm} OFeNCO\ (^2A') \qquad E = 1.1 \text{ kcal/mol} \quad (6)$$

The excitation of Fe(CO)(NO) at $\lambda >$ 470 nm will promote the molecule from the ground state ^{2}A′ into an excited state and apparently form the side-on NO excited state (Fe(CO-[NO])*. Our recent DFT calculations found ^{2}A′ Fe[NO] 20.4 kcal/mol higher than $^2\Delta$ FeNO.[25] Subsequent ultraviolet photolysis restores the initial species and induces rearrangement to the OFeNCO isocyanate.

The intermediate Fe(CO)(NO)$_2$ and Fe(CO)$_2$(NO) complexes are produced on annealing, but the stable 18-electron molecule, Fe(CO)$_2$(NO)$_2$, increased markedly on further annealing and became the dominant product, reactions 7−10. Note that

$$Fe(CO)(NO) + CO \rightarrow Fe(CO)_2(NO) \qquad \Delta E = -28.5 \text{ kcal/mol} \quad (7)$$

$$Fe(CO)(NO) + NO \rightarrow Fe(CO)(NO)_2 \qquad \Delta E = -41.2 \text{ kcal/mol} \quad (8)$$

$$Fe(CO)(NO)_2 + CO \rightarrow Fe(CO)_2(NO)_2 \qquad \Delta E = -42.8 \text{ kcal/mol} \quad (9)$$

$$Fe(CO)_2(NO) + NO \rightarrow Fe(CO)_2(NO)_2 \qquad \Delta E = -55.5 \text{ kcal/mol} \quad (10)$$

adding NO is more exothermic than adding CO to form the iron carbonyl nitrosyl complexes with the same number of ligands (i.e., reactions 3 vs 4, 7 vs 8, and 9 vs 10) as the Fe reaction with NO is more exothermic than with CO (reaction 1 vs 2).

Conclusions

Laser-ablated Fe atoms reacted with CO and NO mixtures during co-deposition in excess argon at 10 K. Weak bands at 1956.3 and 1727.3 cm^{-1} increased in concert on sample annealing and are assigned to the CO and NO stretching modes of the unsaturated Fe(CO)(NO) complex on the basis of the ^{13}CO and ^{15}NO isotopic shifts, and the spectra of isotopic mixtures. The DFT calculations characterized a ^{2}A′ ground state and reproduced the observed frequencies within 1.5% and the isotopic shifts for each ligand within a 0.4 cm^{-1} average. The Fe(CO)(NO) complex converted to Fe(CO)(η^2-NO) on visible photolysis and to the OFeNCO isocyanate on ultraviolet photolysis.

Two isomers, Fe(CO)(NO)$_2$ and Fe(CO)(NO)[NO], were also identified from ^{13}CO and ^{15}NO isotopic substitution and DFT calculations. Both isomers have singlet electronic ground states and Fe(CO)(NO)[NO] is 18.6 kcal/mol higher in energy than Fe(CO)(NO)$_2$. Since one NO is side-coordinated to the Fe atom, the charge distribution on Fe in Fe(CO)(NO)[NO] is more positive, which leads to weaker Fe−C but stronger CO bonds. Further annealing gave the stable 18-electron molecule, Fe(CO)$_2$-(NO)$_2$; the strong carbonyl and nitrosyl stretching modes are in agreement with earlier work and the bending mode region is reported here. DFT calculations reproduce the spectrum and structure of Fe(CO)$_2$(NO)$_2$ quite well.

It is noted in Fe(CO)(NO)$_x$ complexes that as the FeCO angle decreases the δFeCO bending modes blue shift. This is because the 3dπ(Fe)−2π*(CO) interaction is reduced since both the charge distribution on Fe and orientation of the 3dπ(Fe) orbital are strongly perturbed by Fe−NO bonding. As the positive charge on Fe increases, bent FeCO structures are obtained, which is relevant to the bonding in heme−CO adducts.

Acknowledgment. We acknowledge support for this research from the National Science Foundation and the Air Force Office of Scientific Research.

References and Notes

(1) Cotton, F. A.; Wilkinson, G.; Murillo, C. A.; Bochmann, M. *Advanced Inorganic Chemistry*, 6th ed.; Wiley: New York, 1999.

(2) Witteveen, C. F. B.; Giovanelli, J.; Kaufman, S. *J. Biol. Chem.* **1999**, *274*, 29755.

(3) Sakurai, T.; Sakurai, N.; Matsumoto, H.; Hirota, S.; Yamauchi, O. *Biochem. Biophys. Res, Commun.* **1998**, *251*, 248.

(4) Siddhanta, U.; Presta, A.; Fan, B. C.; Wolan, D.; Rousseau, D. L.; Stuehr, D. J. *J. Biol Chem.* **1998**, *273*, 18950.
(5) Moenneloccoz, P.; Devries, S. *J. Am. Chem. Soc.* **1998**, *120*, 5147.
(6) Hieber, W.; Beutner, H. *Z. Anorg. Allg. Chem.* **1963**, *320*, 101.
(7) Chen, H.-W.; Jolly, W. L. *Inorg. Chem.* **1979**, *18*, 2548.
(8) Hedberg, L.; Hedberg, K.; Satija, S. K.; Swanson, B. I. *Inorg. Chem.* **1985**, *24*, 2766.
(9) Kukolich, S. G.; Wallace, D. W.; Wickwire, D. M.; Sickafoose, S. M.; Roehig, M. A. *J. Phys. Chem*. **1993**, *97*, 9317.
(10) Crichton, O.; Rest, A. J. *J. Chem. Soc., Dalton* **1977**, 656.
(11) Gadd, G. E.; Poliakoff, M.; Turner, J. J. *Inorg. Chem.* **1986**, *25*, 3604.
(12) Lombardo, L.; Wege, D.; Wilkinson, S. P. *Aust. J. Chem.* **1974**, *27*, 143.
(13) Morrow, B. A.; Baraton, M. I.; Roustan, J.-L. *J. Am. Chem. Soc.* **1987**, *109*, 7541.
(14) Zhou, M. F.; Chertihin, G. V.; Andrews, L. *J. Chem. Phys.* **1998**, *109*, 10893 (Fe+CO in Ar).
(15) Zhou, M. F.; Andrews, L.; *J. Phys. Chem. A* **1998**, *102*, 10250 (Co+CO).
(16) Zhou, M. F.; Andrews, L. *J. Am. Chem. Soc.* **1998**, *120*, 11499 (Ni+CO).
(17) Zhou, M. F.; Andrews, L. *J. Chem. Phys.* **1999**, *110*, 10370. (Fe+CO in Ne).
(18) Zhou, M. F.; Andrews, L. *J. Phys. Chem. A* **1999**, *103*, 5259 (V, Ti+CO).
(19) Zhou, M. F.; Andrews, L. *J. Phys. Chem. A* **1999**, *103*, 7773 (Co, Rh, Ir+CO).
(20) Kushto, G. P.; Zhou, M. F.; Andrews, L.; Bauschlicher, C. W., Jr. *J. Phys. Chem. A* **1999**, *103*, 1115 (Sc, Ti + NO).
(21) Zhou, M. F.; Andrews, L. *J. Phys. Chem. A* **1999**, *103*, 478 (V+NO).
(22) Zhou, M. F.; Andrews, L. *J. Phys. Chem. A* **1998**, *102*, 7452 (Cr+NO).
(23) Andrews, L.; Zhou, M. F.; Ball, D. W.; *J. Phys. Chem. A* **1998**, *102*, 10041 (Mn+NO).
(24) Andrews, L.; Zhou, M. F.; *J. Phys. Chem. A* **1999**, *103*, 4167 (Mo+NO).
(25) Zhou, M. F.; Andrews, L. *J. Phys. Chem. A* **2000**, *104*, 3915 (Fe, Co, Ni+NO).
(26) Ruschel, G. K.; Nemetz, T. M.; Ball, D. W. *J. Mol. Struct.* **1996**, *384*, 101.
(27) Krim, L.; Manceron, L.; Alikhani, M. E. *J. Phys. Chem.* A **1999**, *103*, 2592.
(28) Burkholder, T. R.; Andrews, L. *J. Chem. Phys*. **1991**, *95*, 8697.
(29) Hassanzadeh, P.; Andrews, L.; *J. Phys. Chem*. **1992**, *96*, 9177.
(30) Jacox, M. E.; Thompson, W. E. *J. Chem. Phys.* **1990**, *93*, 7609.
(31) Frisch, M. J.; Trucks, G. W.; Schlegel, H. B.; Gill, P. M. W.; Johnson, B. G.; Robb, M. A.; Cheeseman, J. R.; Keith, T.; Petersson, G. A.; Montgomery, J. A.; Raghavachari, K.; Al-Laham, M. A.; Zakrzewski, V. G.; Ortiz, J. V.; Foresman, J. B.; Cioslowski, J.; Stefanov, B. B.; Nanayakkara, A.; Challacombe, M.; Peng, C. Y.; Ayala, P. Y.; Chen, W.; Wong, M. W.; Andres, J. L.; Replogle, E. S.; Gomperts, R. R.; Martin, L.; Fox, D. J.; Binkley, J. S.; Defrees, D. J.; Baker, J.; Stewart, J. P.; Head-Gordon, M.; Gonzalez, C.; Pople, J. A. *Gaussian 94*, Revision B.1; Gaussian Inc.: Pittsburgh, PA, 1995.
(32) Perdew, J. P. *Phys. Rev. B* **1986**, *33*, 8822. Becke, A. D. *J. Chem. Phys.* **1993**, *98*, 5648.
(33) McLean, A. D.; Chandler, G. S. *J. Chem. Phys.* **1980**, *72*, 5639. Krishnan, R.; Binkley, J. S.; Seeger, R.; Pople, J. A. *J. Chem. Phys.* **1980**, *72*, 650.
(34) Wachters, H. J. H. *J. Chem. Phys.* **1970**, *52*, 1033. Hay, P. J. *J. Chem. Phys.* **1977**, 66, 4377.
(35) Daoudi, A.; Suard, M.; Berthier, G. *J. Mol. Struct. (THEOCHEM)* **1990**, *210*, 139.
(36) Fournier, R. *J. Chem. Phys*. **1993**, *98*, 8041.
(37) Ricca, A.; Bauschlicher, C. W. Rosi, M. *J. Phys. Chem*. **1994,** *98*, 9498.
(38) Bauschlicher, C. W. *J. Chem. Phys.* **1994**, *100*, 1215.
(39) Castro, M.; Salahub, D. R. Fournier, R.; *J. Chem. Phys*. **1994**, *100*, 8233.
(40) Persson, B. J.; Roos, B. O.; Pierloot, K. *J. Chem. Phys*. **1994**, *101*, 6810.
(41) Adamo, C.; Lelj, F. *J. Chem. Phys.* **1995,** *103*, 10606.
(42) Villalta, P. W.; Leopold, D. G. *J. Chem. Phys*. **1993**, *98*, 7730.
(43) Tanaka, K.; Sakaguchi, K.; Tanaka, T. *J. Chem. Phys.* **1997**, *106*, 2118.
(44) Kuriyan, J.; Wiltz, S.; Karplus, M.; Petsko, G. A. *J. Mol. Biol.* **1986**, *192*, 133.
(45) Chen, X.; Schoenborn, B. *Acta Crystallogr*. **1990,** *B46*, 195. *J. Mol. Biol.* **1991**, *220*, 381.
(46) Quillin, M. L.; Arduini, R. M.; Olson, J. S.; Phillips, G. N., Jr. *J. Mol. Biol.* **1993**, *234*, 140.
(47) Young, F.; Phillips, G. N. Jr. *J. Mol. Biol.* **1996**, *256*, 762.
(48) Spiro, T. G.; Kozolowski, P. M. *J. Am. Chem. Soc*. **1998**, *120*, 4524.
(49) Papai, I.; Stirling, A.; Mink, J.; Nakamoto, K. *Chem. Phys. Lett.* **1998,** *287*, 531.
(50) Ivanov, D.; Sage, J. T.; Keim, M.; Powell, J. R.; Asher, S. A.; Champion, P. M. *J. Am. Chem. Soc.* **1994**, *116*, 4139.
(51) Lim, M.; Jackson, T. A.; Anfinrud, P. A. *Science* **1995**, *269*, 962.
(52) Zhou, M. F.; Liang, B.; Andrews, L. *J. Phys. Chem. A* **1999**, *103*, 2013.
(53) Wang, X.; Zhou, M. F.; Andrews, L. To be published.
(54) Rasko, J.; Solymosi, F. *J. Chem. Soc., Faraday I* **1980**, *76*, 2383.
(55) Hecker, W. C.; Bell, A. T. *J. Catal.* **1984**, *85*, 389.
(56) Kostov, K. L.; Jakob, P.; Rauscher, H.; Menzel, D. *J. Phys. Chem.* **1991**, *95*, 7785.
(57) Miners, J. H.; Bradshaw, A. M.; Gardner, P. *Phys. Chem. Chem. Phys.* **1999**, *1*, 4909.